

Sum and difference frequency mixing of molecular vibrations in a polymer under high-density optical excitation

Izumi Iwakura,^{1,2} Atsushi Yabushita,^{3,4} and Takayoshi Kobayashi^{2,3,4,5,6}

¹*JSPS Research Fellow, 8 Ichibancho, Chiyoda-ku, Tokyo 102-8472, Japan*

²*Department of Applied Physics and Chemistry and Institute for Laser Science, University of Electro-Communications, 1-5-1 Chofugaoka, Chofu, Tokyo 182-8585, Japan*

³*Department of Physics, Graduate School of Science, University of Tokyo, 7-3-1 Hongo, Bunkyo-ku, Tokyo 113-0033, Japan*

⁴*Department of Electrophysics, National Chiao-Tung University, Hsinchu 300, Taiwan*

⁵*ICORP, JST, 4-1-8 Honcho, Kawaguchi, Saitama 332-0012, Japan*

⁶*Institute of Laser Engineering, Osaka University, 2-6 Yamada-oka, Suita, Osaka 565-0971, Japan*

(Received 30 May 2007; published 9 August 2007)

Real-time traces of vibrational amplitude detected by the intensity modulation of electronic transition under high-density excitation with sub-5-fs pulse revealed that a combination tone of the C—C and the C=C stretching modes is generated by the exciton-exciton interaction. They were found to be generated in high quantum number vibrational levels in the ground electronic state after internal conversion from higher excited electronic state created by the Auger process. This indicates that the Auger induced highly excited state results in the fusion of vibrational quantum states. At the same time, parametric difference frequency generation of the vibrational modes takes place in the same process.

DOI: [10.1103/PhysRevB.76.052201](https://doi.org/10.1103/PhysRevB.76.052201)

PACS number(s): 78.66.Qn, 78.47.+p

It has been well known that the lifetimes of molecular excited states and Frenkel excitons are reduced under high-density excitation in aromatic molecular crystals such as anthracene,^{1,2} pyrene,³ fluoranthene,⁴ a charge-transfer complex,⁵ *J* aggregates,⁶ and polymers.^{7–11} The mechanism of the lifetime shortening is well established to be the Auger process, in which one of two neighboring excitations (excited molecules or Frenkel excitons) is excited to a higher excitation (higher electronic excited state in a molecule or an excited exciton state) and the other to the ground state by the transition-dipole–transition-dipole interaction.^{1–4} The higher excitations are expected to relax very rapidly to the lowest excited state or the lowest exciton state, resulting in the shortening of the lifetime of the excitations.^{4,5,8,9} It has not been possible to time resolve the fast relaxation process from the higher excited state generated by the Auger mechanism to the lowest excited singlet state, which includes both electronic relaxation (internal conversion) and vibrational relaxation. The Auger process followed by the relaxation processes has been considered to be nearly instantaneous or beyond the time resolution of the apparatus utilized in the experiments. Usually, the lifetime of the lowest electronic excited state in organic molecules or the Frenkel exciton in organic molecular crystals is in a nanosecond regime in the case that the lowest excited state is allowed. Picosecond or nanosecond pulses had been used in the previous papers, and it was not possible to time resolve the relaxation of the higher excitation via lower excited states to the lowest excited state. It is because the process is considered to take place in a time scale shorter than 100 fs due to the high density of vibronic states near the final state of the Auger excitation. It is of interest to study the relaxation path of the higher excitation generated by the Auger process induced by the high-density excitation. This question arises from the consideration that the higher excited state reached by the Auger process has a different symmetry in the case that the

molecule has parity symmetry. In inversion-symmetric systems, an Auger allowed state generated from the allowed lowest excited state with odd parity is expected to have an even parity, while the final state of the direct transition from the ground state has an odd symmetry. There is the possible difference in the electronic states due to the selection rules between the final state of direct excitation and that due to the Auger process. Therefore, relaxation channel can be different even though both of the electronics states have the same energy because they may be coupled to different vibrational modes selectively excited by the selection rule. The higher excitation is, in general, a vibronically excited state including both higher electronic excitation and vibrational excitation. Hence, there are at least two possible channels of relaxation process. The first one is the relaxation of the electronic energy to the ground state with high vibrational quantum number of various modes in the first stage and then the cooling process of such nonequilibrium state to the thermal state in the ground state. The second channel is the vibrational relaxation followed by electronic relaxation to the ground state.

In this work, sub-5-fs molecular vibrational spectroscopy was applied to study the dynamics of highly excited vibronic states generated by the Auger process under high-density excitation. Real-time observation of the combination tone and difference frequency mode between C—C and C=C stretching modes vibronically coupled to the excitons generated by fusion and fission processes of phonons (molecular vibrational quanta) was successfully made.

In this work, a cast film of polydiacetylene-3-butoxycarbonylmethylurethane on a glass substrate was excited and probed by 5 fs pulses¹² with spectrum extending from 500 to 710 nm at 294 ± 1 K (Fig. 1). Three experiments were performed at various intensities of the pump pulses, 240, 400, and 840 GW/cm², with corresponding pump photon flux of 7.5×10^{29} , 12.5×10^{29} , and 26.8

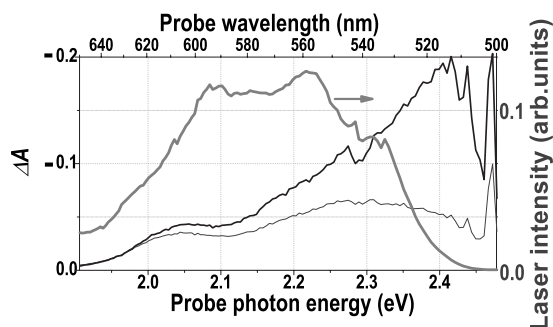


FIG. 1. The difference absorbance ΔA averaged over the delay time range from 0 to 100 fs, when the pump intensities were 400 GW/cm² (black thin curves) and 840 GW/cm² (black thick curves), and the spectrum of the 5 fs laser intensity (a gray thick curve).

$\times 10^{29}$ photons/cm²s and corresponding pump excitation photon density of 7.5×10^{15} , 12.5×10^{15} , and 26.8×10^{15} photons/cm², respectively. The intensity of the probe pulses was maintained to be 120 GW/cm². Figure 1 shows the difference absorption spectra $\Delta A(\lambda)$ averaged over the delay time from 0 to 100 fs.

Figure 2 shows the real-time trace of induced absorbance change probed at ten different probe photon energies at low- and high-density excitations, both of which are highly modulated by the molecular vibration.^{13–15} At high-density excitation, the decay becomes faster and it cannot be fitted to a single exponential function,¹⁶ but can be fitted to the analytic solution including both mono- and bimolecular decay terms.^{1–4,17} When bimolecular quenching of singlet excitons takes place, the time behavior of the exciton density n is expressed by

$$1/n = (\gamma/\alpha + 1/n_0)\exp(\alpha t) - \gamma/\alpha. \quad (1)$$

Here n_0 , α , and γ are the initial value of n , the monomolecular, and bimolecular decay constants, respectively. From the linear relationship between $1/n$ and $\exp(\alpha t)$, α and γ were determined as 5×10^{11} /s and 5.5×10^{-9} cm³/s, respectively. From the latter value, the hopping rate λ of the exciton can be determined as 5.5×10^9 /s, which is faster than that in

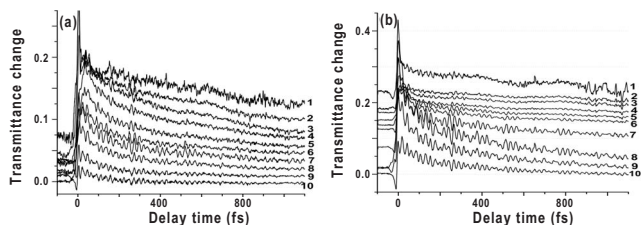


FIG. 2. Real-time trace of induced absorbance change probed at ten different probe photon energies from -100 to 1100 fs, when the pump intensity was (a) 400 GW/cm² and (b) 840 GW/cm². The wavelengths (probe photon energies) of curves 1–10 are as follows: 1, 515 nm (2.406 eV); 2, 530 nm (2.338 eV); 3, 545 nm (2.274 eV); 4, 560 nm (2.213 eV); 5, 575 nm (2.155 eV); 6, 590 nm (2.100 eV); 7, 605 nm (2.048 eV); 8, 620 nm (1.999 eV); 9, 635 nm (1.952 eV); 10, 650 nm (1.907 eV).

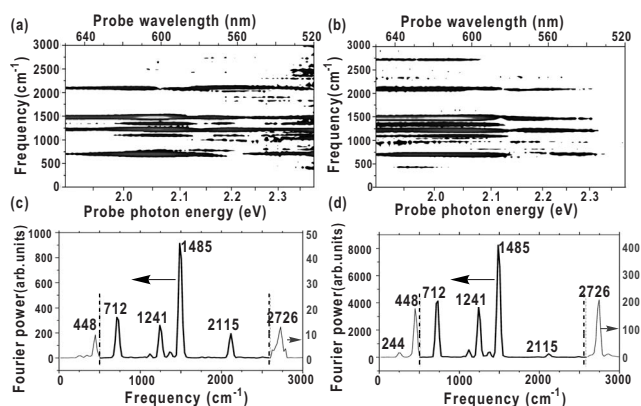


FIG. 3. Two-dimensional Fourier power spectra of the ΔA traces in the delay time ranging from 160 to 1100 fs, when the pump intensities were (a) 400 GW/cm² and (b) 840 GW/cm². Fourier power spectra in the spectral range of probe pulses extending from 1.9 to 2.0 eV where the induced absorptions were observed, when the pump intensities were (c) 400 GW/cm² and (d) 840 GW/cm². Thin lines indicate the Fourier power spectra multiplied by 20.

fluoranthene⁴ (2.2×10^9 /s) probably due to the conjugation. The conjugation hence not only delocalizes the exciton up to about three to four repeat units¹⁸ but also helps the exciton hopping.

Figures 3(a) and 3(b) show the probe wavelength dependence of the Fourier power spectrum of the real-time traces $\Delta A(t)$ in the delay time ranging from 160 to 1100 fs. The symmetric C—C stretching mode (ν_{sC-C}) was observed at 1241 cm⁻¹ (mode 2). An intense band at 1485 cm⁻¹ (mode 3) was assigned to the C=C stretching mode ($\nu_{C=C}$). A peak at 2726 cm⁻¹ (mode 4) can be assigned to the combination tone between the ν_{sC-C} (1241 cm⁻¹) and the $\nu_{C=C}$ (1485 cm⁻¹).¹⁰ Peaks at 244, 448, 712, and 2116 cm⁻¹ were assigned to C—C=C bending mode ($\rho_{C-C=C}$), C—C≡C—C wagging mode ($\omega_{C-C≡C-C}$), C—C=C torsion mode ($\tau_{C-C=C}$), and C≡C stretching mode ($\nu_{C≡C}$),^{12,19} respectively. As seen in Fig. 1, the absorbance change ΔA does not depend on the pump intensity and is almost constant in the spectral range of probe pulses extending from 1.9 to 2.0 eV. However, the absorbance changes increased almost proportionally to the pump intensity in the spectral range from 2.0 to 2.4 eV. This result shows that the combination tone appeared on the excitation from the lowest excitation (exciton state) to the higher excitation (excited state of exciton). Fourier power spectrum in the spectral range of the induced absorption is shown in Figs. 3(c) and 3(d). In these figures, the amplitudes of ν_{sC-C} , $\nu_{C=C}$, $\omega_{C-C≡C-C}$, and $\tau_{C-C=C}$ increased nearly proportionally to the pump intensity (see also Fig. 4). On the other hand, the amplitudes of the peaks at 244 and 2726 cm⁻¹ were found to be superlinear to the pump intensity. In addition, the frequency of the peak at 244 cm⁻¹ (mode 1) is exactly equal to the difference between 1485 and 1241 cm⁻¹. Previous paper reported that ν_{sC-C} (1241 cm⁻¹) and $\nu_{C=C}$ (1485 cm⁻¹) were coupled via in-plane bending mode in the main chain (244 cm⁻¹).^{13,20} It indicates that the coupling among the relevant three modes is enhanced on high-density excitation.

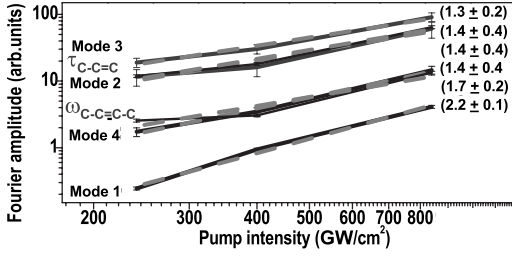


FIG. 4. Relation between the pump intensity and Fourier amplitudes in the spectral range of probe pulses extending from 1.9 to 2.0 eV. Six modes correspond to mode 2 ($\nu_{\text{C-C}} = 1241 \text{ cm}^{-1}$), mode 3 ($\nu_{\text{C-C}} = 1485 \text{ cm}^{-1}$), mode 1 ($\nu_{\text{C-C}} - \nu_{\text{S-C-C}} = 244 \text{ cm}^{-1}$), mode 4 ($\nu_{\text{C-C}} + \nu_{\text{S-C-C}} = 2726 \text{ cm}^{-1}$), $\omega_{\text{C-C=C-C}}$ (448 cm^{-1}), and $\tau_{\text{C-C=C}}$ (712 cm^{-1}).

There are three possible channels, which can be the excitation channel to leads to the highly excited vibrational levels under high-density excitation due to the third-order nonlinear mechanisms. The first and second channels are simultaneous (photon-photon nonlinearity) and sequential (exciton-photon nonlinearity) photoexcitations, respectively. The third one is excitation by the Auger process induced by biexciton interaction (exciton-exciton nonlinearity).⁵ If the first and second processes are the cases, the initial absorbance change saturates but decay dynamics does not change even when the pump intensity is increased, but only the dynamic signal amplitude of the electronic transition is increased under high-density excitation. The decay dynamics was dependent on pump intensity as discussed before; therefore, the possibility of the process can be ruled out, and we find that the excitation by the Auger process is the case.

Figure 5 shows the probe photon energy dependence of the amplitudes of modes 1, 2, 3, and 4 and the product of modes 2 and 3. Amplitudes in the photon energies between 1.95 and 2.05 eV are relatively higher than in other photon energies over all of the modes. The product of the amplitudes of modes 2 and 3 was found to be in agreement with that of the modes 1 and 4. This finding also confirms that the combination tone (mode 4) and the difference frequency (mode 1) are generated by the collision of the vibronic excitations (vibronic exciton) of modes 2 and 3. Here, the dynamics of

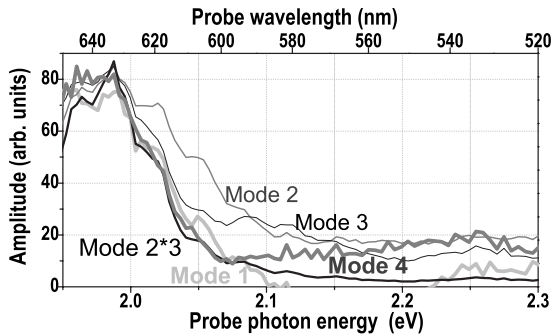


FIG. 5. Dependence on the probe photon energy from 1.95 to 2.3 eV of the amplitudes of the five modes with the $\nu_{\text{S-C-C}} = 1241 \text{ cm}^{-1}$ (mode 2), the $\nu_{\text{C-C}} = 1485 \text{ cm}^{-1}$ (mode 3), the combination tone 244 cm^{-1} (mode 1), 2726 cm^{-1} (mode 4), and $1241 * 1485 \text{ cm}^{-1}$ (mode 2* mode 3).

the relevant four modes is to be discussed. Modes 2 and 3 are the modes directly photogenerated by femtosecond laser and modes 1 and 4 are generated through the Auger process. Then, the dynamics of the envelope of signal amplitudes $c_i(\lambda, t)$ of modes i ($i=1, 2, 3,$ and 4) probed at wavelength λ can be described as follows:

$$\frac{dc_i(\lambda, t)}{dt} = a_i I(\lambda, t) - k_i c_i(\lambda, t), \quad i = 2, 3, \quad (2)$$

$$\frac{dc_j(\lambda, t)}{dt} = b_j c_2(\lambda, t) c_3(\lambda, t) - k_j c_j(\lambda, t), \quad j = 1, 4. \quad (3)$$

Instantaneous amplitude of each mode is given by $c_i(\lambda, t) e^{i(\omega_i t + \phi_i)}$ with frequency ω_i and initial phase ϕ_i . Here, $I(t)$ is the pump laser intensity. The parameters a_i ($i=2, 3$) and b_j ($j=1, 4$) represent the generation efficiency for the relevant modes via direct photoexcitation and the Auger process, respectively. k_i ($i=1, 2, 3,$ and 4) are the vibrational amplitude decay rates of the corresponding modes. These equations can be solved as follows:

$$C_i(t) = a_i \int_{-\infty}^t I(t') e^{-k_i(t-t')} dt', \quad i = 2, 3, \quad (4)$$

$$C_j(t) = b_j \int_{-\infty}^t c_2(\lambda, t') c_3(\lambda, t') e^{-k_j(t-t')} dt', \quad j = 1, 4. \quad (5)$$

The rates k_i were determined as $k_1^{-1} = 220 \text{ fs}$, $k_2^{-1} = 1600 \text{ fs}$, $k_3^{-1} = 1600 \text{ fs}$, and $k_4^{-1} = 450 \text{ fs}$ from the experimental results. From Eqs. (4) and (5), it is expected that the pump pulse intensity dependences of modes 2 and 3 are linear, while those of modes 1 and 4 are quadratic. Figure 4 shows the pump intensity dependence of the signal intensity, and powers s of the intensity dependence I^s for four modes were determined as $s_1 = 2.2 \pm 0.1$, $s_2 = 1.4 \pm 0.4$, $s_3 = 1.3 \pm 0.2$, and $s_4 = 1.7 \pm 0.2$, respectively. These values are consistent with the above expectation. The deviations of the values of s_1 and s_4 from 2 may be due to the effects of higher-order excitation and saturation, respectively. The deviations of the values of s_2 and s_3 from unity are probably due to that the processes of $\omega_2 = \omega_3 - \omega_1$ and $\omega_3 = \omega_4 - \omega_2$ are also taking place after the generation of ω_3 and ω_4 .

Modulation amplitudes of electronic transitions induced by molecular vibration $c_1(\lambda, t)$ and $c_4(\lambda, t)$ are expected to be proportional to $c_2(\lambda, t) c_3(\lambda, t)$ because of the short lifetimes. Since the decay time of the modulation of each mode is independent of probe wavelength, the integrated modulation amplitudes $C_k(\lambda) = \int_{t_1}^{t_2} c_k(\lambda, t) dt$, ($k=1, 2, 3, 4$) of these four modes over the probe time range ($t_1=0 \text{ fs}$, $t_2=1100 \text{ fs}$) are expected to satisfy the relation $C_i(\lambda) \propto C_2(\lambda) C_3(\lambda)$ ($i=1, 4$). Therefore, the widths of $C_1(\lambda)$ and $C_4(\lambda)$ are narrower than those of $C_2(\lambda)$ and $C_3(\lambda)$. It agrees with the experimental results that the spectral widths of the modes 1 and 4 are narrower than those of modes 2 and 3 as seen in Fig. 5.

In the present Brief Report, we clearly demonstrated experimentally that the following reactions take place in which

electric-dipole–electric-dipole energy-transfer interaction in the Auger process is associated with the exchange of vibration quanta:

$$(E_1, n_1, n_2, n_3, n_4) + (E_1, n'_1, n'_2, n'_3, n'_4) \rightarrow (E_n, n_1 + 1, n_2, n_3, n_4) + (G, n'_1, n'_2 - 1, n'_3 - 1, n'_4), \quad (6)$$

$$(E_1, n_1, n_2, n_3, n_4) + (E_1, n'_1, n'_2, n'_3, n'_4) \rightarrow (E_n, n_1, n_2, n_3 + 1, n_4 + 1) + (G, n'_1 - 1, n'_2, n'_3, n'_4). \quad (7)$$

Here (A, n_1, n_2, n_3, n_4) represents the electronic state A ($=G, E_1$, or E_n) in the ground state (G), the lowest excited state (E_1), and higher excited state (E_n) coupled with molecular vibrations with n_1, n_2, n_3 , and n_4 quanta of modes $\omega_1, \omega_2, \omega_3$, and ω_4 , respectively. The state is a linear combination of such vibronic states with different sets of vibrational quanta (n_1, n_2, n_3, n_4) . Main contributions of n_i ($i=1, 2, 3$, and 4) are 0 or 1. Processes (6) and (7) are sum and difference frequency generations of molecular vibrations. The latter is a parametric process, which is extensively utilized in nonlinear optics.

If two excitons collide followed by the ‘‘Auger process,’’ one of the excitons is ionized with the expense of the energy of the other exciton¹ or the electronic energy of an exciton is transferred to the other exciton by the ‘‘Förster energy transfer,’’ resulting in the higher excited state.^{2–4} In this work, we found that the energies of molecular vibrations were also

transferred at the same time with the transfer of the electronic energies.

The sum of the molecular vibration frequencies of modes 2 and 3 was exactly equal to the observed molecular vibration frequency of the mode 4 referred to the product of modes 2 and 3. It clarifies that the sum of molecular vibration energies is conserved before and after the collisions of vibronic excitons. It was discovered that the molecular vibration and electronic energies are conserved independently even though there are many possible vibrational levels in the vibration modes. Thus, it was discovered from our direct observation of exchange of vibrational quanta in the Auger process that efficient vibrational energy exchange takes place for modes satisfying sum-frequency or parametric interaction condition.

In conclusion, we discovered that highly anharmonic molecular vibration is induced on high-density excitation by the Auger process for the molecular vibrational modes fused to generate the combination tone and difference frequency mode. The latter is the parametric process for the molecular vibrational modes and is the molecular vibrational version of frequency conversion.

This work was supported by JSPS Research Foundation for Young Scientists, ICORP program of JST, the grant MOE ATU Program in NCTU, and a Grant-in-Aid for Science Research in a Priority Area ‘‘Super-Hierarchical Structures’’ from the Ministry of Education, Culture, Sports, Science and Technology, Japan.

¹A. Bergman, M. Levine, and J. Jortner, *Phys. Rev. Lett.* **18**, 593 (1967).

²T. Kobayashi and S. Nagakura, *Mol. Cryst. Liq. Cryst.* **26**, 33 (1974).

³A. Inoue, K. Yoshihara, and S. Nagakura, *Bull. Chem. Soc. Jpn.* **45**, 1973 (1972).

⁴T. Kobayashi and S. Nagakura, *Mol. Phys.* **24**, 695 (1972).

⁵Z. Z. Ho and N. Peyghambarian, *Chem. Phys. Lett.* **148**, 107 (1988).

⁶K. Minoshima, M. Taiji, K. Misawa, and T. Kobayashi, *Chem. Phys. Lett.* **218**, 67 (1994).

⁷S. Adachi, V. M. Kobryanskii, and T. Kobayashi, *Phys. Rev. Lett.* **89**, 027401 (2002).

⁸A. Terasaki, M. Hosoda, T. Wada, H. Tada, A. Koma, A. Yamada, H. Sasabe, A. F. Garito, and T. Kobayashi, *J. Phys. Chem.* **96**, 10534 (1992).

⁹V. S. Williams, S. Mazumdar, N. R. Armstrong, Z. Z. Ho, and N. Peyghambarian, *J. Phys. Chem.* **96**, 4500 (1992).

¹⁰T. Kobayashi, T. Fuji, N. Ishii, and H. Goto, *J. Lumin.* **94-95**, 667 (2001).

¹¹V. Gulbinas, M. Chachisvilis, L. Valkunas, and V. Sundstrom, *J. Phys. Chem.* **100**, 2213 (1996).

¹²A. Baltuska and T. Kobayashi, *Appl. Phys. B: Lasers Opt.* **75**, 427 (2002).

¹³M. Ikuta, Y. Yuasa, T. Kimura, H. Matsuda, and T. Kobayashi, *Phys. Rev. B* **70**, 214301 (2004).

¹⁴J. Y. Bigot, T. A. Pham, and T. Barisien, *Chem. Phys. Lett.* **259**, 469 (1996).

¹⁵Q. Wang, R. W. Schoenlein, L. A. Petearnu, R. A. Mathies, and C. V. Shank, *Science* **266**, 422 (1994).

¹⁶T. Kobayashi, M. Yoshizawa, U. Stamm, M. Taiji, and M. Hasegawa, *J. Opt. Soc. Am. B* **7**, 1558 (1990).

¹⁷T. Kobayashi and S. Nagakura, *Mol. Phys.* **23**, 1211 (1972).

¹⁸H. Tanaka, M. Inoue, and E. Hanamura, *Solid State Commun.* **103-107**, 63 (1987).

¹⁹T. Kobayashi, A. Shirakawa, H. Matsuzawa, and H. Nakanishi, *Chem. Phys. Lett.* **321**, 385 (2000).

²⁰A. Vierheilg, T. Chen, P. Waltner, W. Kiefer, A. Materny, and A. H. Zewail, *Chem. Phys. Lett.* **312**, 349 (1999).